

Proceedings of the Eleventh International Conference on  
Engineering Computational Technology  
Edited by B.H.V. Topping and P. Iványi  
Civil-Comp Conferences, Volume 2, Paper 11.2  
Civil-Comp Press, Edinburgh, United Kingdom, 2022, doi: 10.4203/ccc.2.11.2  
©Civil-Comp Ltd, Edinburgh, UK, 2022

## **An improved 2D-MITC4 element**

**H.G. Choi and P.S. Lee**

**Department of Mechanical Engineering, Korea Advanced  
Institute of Science and Technology, Daejeon, Republic of Korea**

### **Abstract**

Recently, the 2D-MITC4 element has been developed for analysis of 2D solid problems. In this paper, we introduce a new formulation of an improved 2D-MITC4 element. The improved 2D-MITC4 element passes the basic test (isotropy, patch and zero energy modes tests) and shows significantly enhanced convergence behavior in both regular and distorted meshes.

**Keywords:** finite element analysis, MITC method, mesh distortion, numerical integration, 4-node 2D solid element.

### **1 Introduction**

The mixed interpolation of tensorial components (MITC) method has been extensively employed to develop various solid and structural elements [1-8] since it was first proposed to reduce transverse shear locking for a 4-node quadrilateral shell element [9]. Finite elements based on the MITC method effectively alleviate various types of locking without using additional degrees of freedom and do not show spurious instabilities in both linear and nonlinear analyses.

Recently, the MITC method was applied to develop the 4-node solid element for two-dimensional solid problems [10]. The assumed strain field of the 2D-MITC4 element is constructed to reduce in-plane shear locking. The element provides highly accurate solutions comparable to the incompatible modes element without spurious instabilities that incompatible modes element shows [11]. While the element shows

almost optimal convergence behavior in regular meshes, its performance deteriorates in distorted meshes [12-15]. The goal of this study is to enhance the convergence behavior of the 2D-MITC4 element in distorted meshes while preserving the promising properties of the MITC method aforementioned. The formulation of the improved 2D-MITC4 element is briefly presented.

## 2 Methods

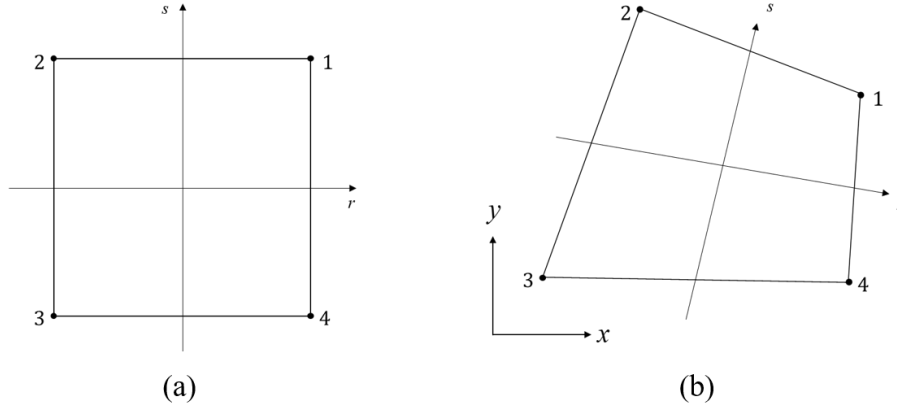


Figure 1: A 4-node quadrilateral element in (a) a natural coordinate system and (b) a global cartesian coordinate system.

Considering the 4-node element in **Fig.1**, the geometry and displacement of the standard 4-node quadrilateral 2D solid element are interpolated by [1,9,10],

$$\mathbf{x} = \sum_{i=1}^4 h_i(r,s) \mathbf{x}_i \quad \text{with } \mathbf{x}_i = [x_i \quad y_i]^T, \quad (1)$$

$$\mathbf{u} = \sum_{i=1}^4 h_i(r,s) \mathbf{u}_i \quad \text{with } \mathbf{u}_i = [u_i \quad v_i]^T, \quad (2)$$

where  $\mathbf{x}_i$  and  $\mathbf{u}_i$  are position and displacement vectors of the  $i$ th node, respectively, and  $h_i$  is the bilinear shape function corresponding to the  $i$ th node. The shape functions are given as

$$h_1(r,s) = \frac{1}{2}(1+r)(1+s), \quad h_2(r,s) = \frac{1}{2}(1-r)(1+s), \quad (3)$$

$$h_3(r,s) = \frac{1}{2}(1-r)(1-s), \quad h_4(r,s) = \frac{1}{2}(1+r)(1-s). \quad (4)$$

In the formulation of the 2D-MITC4 element, the strain components are expressed by employing constant base vectors instead of covariant strain components

$$\mathbf{e} = \hat{e}_{ij} (\hat{\mathbf{g}}^i \otimes \hat{\mathbf{g}}^j) \quad \text{with } i = 1, 2, \quad (5)$$

in which  $\hat{\mathbf{g}}^i$  is the contravariant base vector evaluated at the element center.

Then, using the tying points (A)-(E) as shown in **Fig. 2**, the assumed strain field is constructed as

$$\hat{e}_{rr}^{AS} = \hat{e}_{rr}^{(E)} + \frac{\lambda(r,s)}{2d} s (\hat{e}_{rr}^{(A)} - \hat{e}_{rr}^{(B)}), \quad (6)$$

$$\hat{e}_{ss}^{AS} = \hat{e}_{ss}^{(E)} + \frac{\lambda(r,s)}{2d} r (\hat{e}_{ss}^{(C)} - \hat{e}_{ss}^{(D)}), \quad (7)$$

$$\hat{e}_{rs}^{AS} = \hat{e}_{rs}^{(E)}, \quad (8)$$

in which  $d$  denotes the distance between tying points (A)-(D) and the element center, and  $\lambda$  is the ratio of the determinants of the Jacobian matrices. A new assumed strain field is obtained by taking the distance close to the element center.

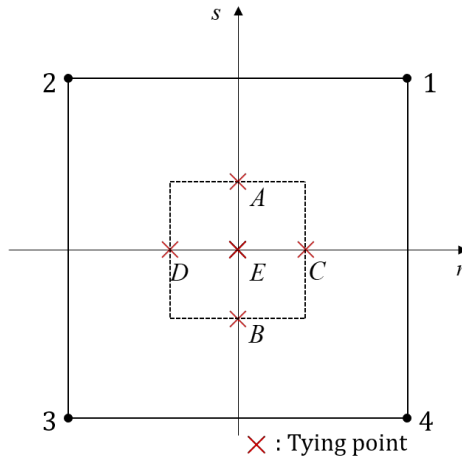


Figure 2: Tying points used for the assumed strain field of the improved 2D-MITC4 element.

In addition, to enhance the performance of the element, when evaluating the stiffness matrix of the improved 2D-MITC4 element, we adjust the positions of integration points as follows:

$$\mathbf{K}^e = \sum_{i=1}^2 \sum_{j=1}^2 w_i w_j \mathbf{f}(\zeta_i', \zeta_j') \quad \text{with} \quad \zeta_i' = \gamma \zeta_i, \quad \gamma = 1 - \left( \frac{\hat{\mathbf{g}}_r \cdot \hat{\mathbf{g}}_s}{|\hat{\mathbf{g}}_r| |\hat{\mathbf{g}}_s|} \right)^2 \quad (9)$$

in which  $\zeta_i$  and  $w_i$  are standard two-point Gauss integration point and the corresponding weight, respectively,  $\gamma$  is the adjusting parameter,  $\zeta_i'$  is the adjusted integration point, and  $\hat{\mathbf{g}}_i$  is the covariant base vectors evaluated at the element center.

### 3 Results

The improved 2D-MITC4 element passes all basic tests including zero energy mode, isotropy and patch tests. To investigate the performance of the improved 2D-MITC4 element, the clamped square plate is solved as shown in **Fig. 3 (a)**. The plate is supported at left edge and is subjected to in-plane moment at the right edge. The plane

stress condition is employed with Young's modulus  $E=1$  and Poisson's ratio  $\nu=0.3$ . For the solutions we use distorted meshes with  $N \times N$  elements ( $N=2, 4, 8$  and 16) as shown in **Fig. 3(b)**.

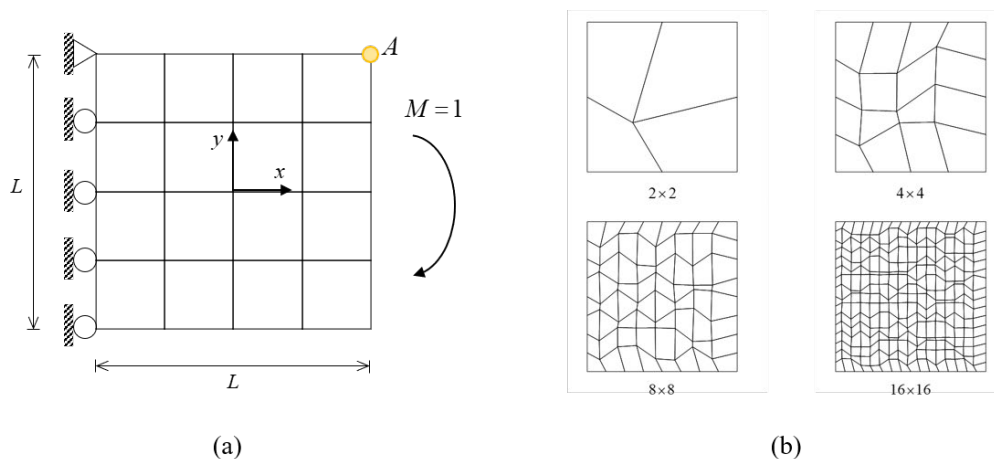


Figure 3: Clamped square plate: (a) the square plate ( $L=2$ ) subjected to in-plane moment and (b) distorted meshes used.

The relative error is calculated using the reference strain energy obtained by a  $64 \times 64$  mesh of 9-node solid elements. The element size in the convergence curves is denoted as  $h=1/N$ . **Fig. 4** shows the convergence curves with the optimal convergence rate. **Tables 1** and **2** give the relative errors in horizontal and vertical displacements at point  $A$ . The results show that the improved 2D-MITC4 element provides more accurate solutions than both the standard 4-node solid element and the original 2D-MITC4 element.

N	Q4	2D-MITC4	Improved
2	19.12%	7.59%	11.53%
4	6.92%	3.96%	0.44%
8	2.28%	1.38%	0.25%
16	0.78%	0.34%	0.12%

Table 1: Relative errors in the horizontal displacement ( $|u_{ref} - u_h| / u_{ref} \times 100$ ) at the point  $A$ .

## 4 Conclusions and Contributions

In this paper, the formulation of the improved 2D-MITC4 element was presented for the two-dimensional analysis of problems in solid mechanics. Since the stiffness of the original 2D-MITC4 element is overestimated when the element is distorted, the performance of the element is deteriorated. A simplification of the original 2D-

MITC4 element is performed and the modified integration rule was proposed to make the element insensitive to element distortion. The element passes all basic tests and provides the enhanced predictive capability especially in distorted meshes. This element could be applicable for improving the membrane behavior of the 4-node plate and shell elements.

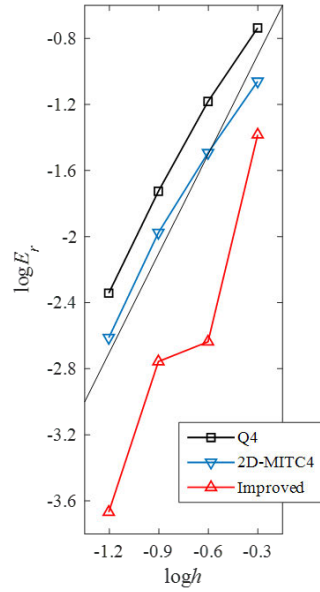


Figure 4: Convergence curves for the square plate problem. The bold line denotes the optimal convergence rate.

N	Q4	2D-MITC4	Improved
2	23.29%	6.96%	9.53%
4	6.08%	2.95%	1.37%
8	1.93%	1.04%	0.09%
16	0.83%	0.42%	0.08%

Table 2: Relative errors in the vertical displacement ( $|v_{ref} - v_h| / v_{ref} \times 100$ ) at the point  $A$ .

## Acknowledgements

This work was supported by the National Research Foundation of Korea (NRF) grant funded by the Korea government (MSIT) (No. NRF-2018R1A2B3005328).

## References

- [1] Ko Y, Lee PS, Bathe KJ. The MITC4+ shell element in geometric nonlinear analysis. *Comput Struct* 2017;185:1–14.
- [2] Bucalem ML, Bathe K -J. Higher-order MITC general shell elements. *Int J Numer Methods Eng* 1993;36:3729–54.
- [3] Bathe KJ, Lee PS, Hiller JF. Towards improving the MITC9 shell element. *Comput Struct* 2003;81:477–89.
- [4] Lee PS, Bathe KJ. Development of MITC isotropic triangular shell finite elements. *Comput Struct* 2004;82:945–62.
- [5] Beirão da Veiga L, Chapelle D, Paris Suarez I. Towards improving the MITC6 triangular shell element. *Comput Struct* 2007;85:1589–610.
- [6] Lee Y, Lee PS, Bathe KJ. The MITC3+ shell element and its performance. *Comput Struct* 2014;138:12–23.
- [7] Jeon HM, Lee PS, Bathe KJ. The MITC3 shell finite element enriched by interpolation covers. *Comput Struct* 2014;134:128–42.
- [8] Ko Y, Lee PS. A 6-node triangular solid-shell element for linear and nonlinear analysis. *Int J Numer Methods Eng* 2017;111:1203–30.
- [9] Dvorkin EN, Bathe K. A continuum mechanics based four-node shell element for general non-linear analysis. *Eng Comput* 1984;1:77–88.
- [10] Ko Y, Lee PS, Bathe KJ. A new 4-node MITC element for analysis of two-dimensional solids and its formulation in a shell element. *Comput Struct* 2017;192:34–49.
- [11] Sussman T, Bathe KJ. Spurious modes in geometrically nonlinear small displacement finite elements with incompatible modes. *Comput Struct* 2014;140:14–22.
- [12] Lee N-S, Bathe K-J. Effects of element distortions on the performance of isoparametric elements. *Int J Numer Methods Eng* 1993;36:3553–76.
- [13] Macneal RH. A theorem regarding the locking of tapered four-noded membrane elements. *Int J Numer Methods Eng* 1987;24:1793–9.
- [14] Panasz P, Wisniewski K, Turska E. Reduction of mesh distortion effects for nine-node elements using corrected shape functions. *Finite Elem Anal Des* 2013;66:83–95.
- [15] MacNeal RH. Toward a defect-free four-noded membrane element. *Finite Elem Anal Des* 1989;5:31–7.